Liquid Crystals
Publication details, including instructions for authors and subscription information:
http://www.informaworld.com/smpp/title~content=t713926090

Viscoelastic behaviour of the SmC* phase

Z. Hammami[a]; T. Othman[a]; A. Gharbi[a]; H. T. Nguyen[b]
[a] Laboratoire de Physique de la Matière Molle, Faculté des Sciences de Tunis, 1060 Belvédère, Tunis-Tunisie [b] Centre de Recherche Paul Pascal, F-33600 Pessac Cedex, France

To cite this Article Hammami, Z. , Othman, T. , Gharbi, A. and Nguyen, H. T.(2005) 'Viscoelastic behaviour of the SmC* phase', Liquid Crystals, 32: 5, 579 — 584

To link to this Article: DOI: 10.1080/02678290500115823

URL: http://dx.doi.org/10.1080/02678290500115823

Liquid Crystals, Vol. 32, No. 5, May 2005, 579–584

Viscoelastic behaviour of the SmC* phase

Z. HAMMAMI†, T. OTHMAN*†, A. GHARBI† and H.T. NGUYEN‡
†Laboratoire de Physique de la Matière Molle, Faculté des Sciences de Tunis, 1060 Belvédère, Tunis-Tunisie
‡Centre de Recherche Paul Pascal, Ave. A. Schweitzer, F-33600 Pessac Cedex, France

(*Received 5 May 2004; in final form 22 December 2004; accepted 22 December 2004*)

Using a light scattering technique at a fixed temperature, we have investigated viscoelastic behaviour exhibited by the ferroelectric smectic phase (SmC*) of C_8tolane in a homeotropic orientation. Experiments were performed in backward and forward scattering geometries that allowed us to deduce separately orientational diffusivities k_3/η and k_+/η corresponding to the Goldstone mode. The k_3/η value measured in the SmC* phase is about 100 times higher than in the SmC_A^* phase exhibited by the same liquid crystal compound. The factor 100 may be attributed in great part to the molecular arrangement mode in adjacent smectic layers. However k_+/η measured in the SmC* phase is in the same order of magnitude as those measured previously in SmC_A^* phases.

1. Introduction

Based on a symmetry argument, Meyer [1] announced the possibility of ferroelectricity in liquid crystals consisting of rod-like molecules. When the constituent molecules are chiral (i.e. molecules are different from their mirror image) a helical structure known as the smectic C* (SmC*) phase is formed instead of the smectic C (SmC). In the SmC* phase, the average direction of molecules is tilted at an angle θ with respect to the normal to the layers and precesses with a period p when moving on from one layer to the next. Note that the period p is in the same order of magnitude as the wavelength range of visible light, and is much larger than the interlayer distance, so that the SmC* phase can be considered as a continuous helical system. One can thus easily conclude that the unit cell characterizing the helical structure in the SmC* phase is a single layer.

In 1983 the Orsay group [2] synthesized the chiral product 1-methyl-heptyl terephtalidene-bis-aminocinnmate (MHTAC), which exhibited new smectic phases that were identified by optical microscopy, differential thermal analysis and X-ray diffraction. One of these phases exhibits a liquid order in the layers, where molecules are tilted by an angle θ with respect to the normal to the layers; but in adjacent layers the molecules are tilted in opposite directions. This chevron structure was identified by Galerne *et al.* [3] on analysing a thin film of MHTAC liquid crystal. At around the same time, the Tokyo group first reported the antiferroelectric nature of chiral smectic phases [4].

The same experiments performed on 4-(1-methylheptyloxycarbonyl)phenyl 4′-octyloxybiphenyl-4-carboxylate (MHPOB) allowed Bahr [5, 6] to confirm the alternated structure (or anticlinic structure) observed and identified by Galerne in MHTAC liquid crystal. These phases are called the antiferroelectric smectic phase (SmC_A^*) because the direction of the local spontaneous polarization of neighbouring layers is reversed by nearly 180° on moving along the layer normal. The helical structure observed in these phases is formed by a double-twisted helical structure, with two ferroelectric helices geared into each other. In the SmC_A^* phase the unit cell is formed by two adjacent layers that give an antiferroelectric system. Therefore, because of the difference between the molecular arrangement modes observed in SmC* and SmC_A^* phases, one may expect a difference in their viscoelastic behaviour.

Furthermore we should note that since their discovery, and because of the possibility of their application in high technological devices, ferroelectric liquid crystals have attracted the efforts of many theoreticians and experimentalists to define certain optical and thermodynamic properties. For example, the determination of the orientational diffusivity (ratio of viscosity coefficient to elastic constant) is very useful in the application of ferroelectric liquid crystals to optical instruments such as the light modulator [7, 8] and other optical devices.

Our contribution in this research field is to use the quasi-elastic light scattering technique to measure

---

*Corresponding author. Email: tahar.othman@fst.rnu.tn

ISSN 0267-8292 print/ISSN 1366-5855 online © 2005 Taylor & Francis Group Ltd
http://www.tandf.co.uk/journals
DOI: 10.1080/02678290500115823

orientational diffusivities associated with thermal fluctuations of the tilt and azimuthal angles in SmC* and SmC$_A^*$ phases, and then to deduce information on the viscoelastic behaviour of these liquid crystal phases.

In previous work, we investigated ferro- and antiferro-electric phases corresponding to C$_{11}$thiobenzoate and C$_8$tolane liquid crystals that belong to the thiobenzoate and tolane series respectively [9]. In the C$_{11}$thiobenzoate case we investigated both SmC$_A^*$ and SmC* phases, but for C$_8$tolane, experiments were performed only in the SmC$_A^*$ phase. The results showed that, on the one hand, SmC$_A^*$ and SmC* phases of the same liquid crystal compound (C$_{11}$thiobenzoate) exhibit different viscoelastic behaviour, and on the other hand, SmC$_A^*$ phases of different liquid crystal compounds (C$_{11}$thiobenzoate and C$_8$tolane) exhibit similar viscoelastic behaviour despite the difference between molecular tails and constitutional atoms. This difference was attributed largely to the molecular arrangement mode that probably affects curvature elastic constants and viscosity coefficients.

The results presented in this paper may support the arguments and conclusions [9] concerning the effect of the molecular arrangement mode on viscoelastic behaviour in ferro- and antiferro-electric phases. In §2 we recall some theoretical predictions concerning thermal fluctuations of the molecular average direction. In §3, we describe experimental techniques and the material investigated; experimental results and discussion are presented in §4.

2. Theory

In liquid crystals, as in all other materials, molecules undergo thermal fluctuations above absolute zero temperature. These fluctuations can be divided into two categories: the fast mode corresponds to rotational degrees of freedom of the individual molecules; the slow fluctuations correspond to collective excitations of the molecules. Important physical properties (phase transition, light scattering) and applications (switching process) can therefore be deduced from the study of the collective excitations dynamics in the liquid crystalline phase. Among the many experimental techniques used to study the dynamics of molecular fluctuations, we cite the quasi-elastic light scattering — more precisely the light beating — technique as the suitable technique to study the dynamics of the slow fluctuations. This experimental technique consists of measuring the autocorrelation function associated with the photocurrent corresponding to the light scattered by orientational fluctuations. Orientational diffusivities linked to curvature elastic constants and viscosity coefficients can be then deduced. Conclusions on vicoelastic behaviour of the liquid crystals may then be reached [10–12].

In the SmC* phase, the collective fluctuations of the molecular direction can be decomposed into the fluctuations of the tilt angle magnitude and rotation on the cone around the normal smectic layers. The first mode, usually called the amplitude (or soft) mode, involves a change in layer spacing. The second mode, known to be a slow fluctuation mode and called the phasing (or Goldstone) mode corresponds to fluctuation of the azimuth angle. Furthermore, we should note that the soft mode involving change in layer spacing costs more energy for thermal excitations. It can therefore only be observed near the transition temperature. Far away from the transition, this mode is suppressed by the Goldstone mode [13].

Fluctuations of the helical structure give rise to an inhomogeneous dielectric tensor $\varepsilon(\vec{r})$. The fluctuate part $\delta\varepsilon(\vec{r})$ of this tensor contains two terms with spatial period $q_0=2\pi/p$ and $2q_0$, where p is the pitch of the macroscopic helical structure. Consequently, in a light scattering experiment the light scattered by collective excitations is centred on q_0 and $2q_0$. Based on Landau thermodynamic potential describing the SmA to SmC* transition, Drevensek *et al.* [14] have established for the amplitude and the phase modes the relaxation times τ_a and τ_p, respectively given by the following expressions:

$$\frac{1}{\tau_\mathrm{a}}=\frac{2\alpha}{\eta}(T-T_\mathrm{c})+\frac{k_3}{\eta}(q_\mathrm{s}\pm 2q_0)^2+\frac{k_+}{\eta}q_\perp^2 \tag{1}$$

$$\frac{1}{\tau_\mathrm{p}}=\frac{k_3}{\eta}(q_\mathrm{s}\pm 2q_0)^2+\frac{k_+}{\eta}q_\perp^2 \tag{2}$$

where α is a positive constant, T_c is the transition temperature, η represents an orientational viscosity coefficient; k_3 is a curvature elastic constant associated with twist deformation, and $k_+=(k_1+k_2)/2$ where k_1 and k_2 are curvature elastic constants analogous to the splay and bend constants of a nematic phase. q_s and $q_\perp$ are the parallel and normal components, respectively, of the scattering wave vector with respect to the helix axis.

Furthermore, we should note that according to expressions (1) and (2) the frequency dispersion branch corresponding to the phase mode has a zero relaxation rate at $q_\mathrm{s}=2q_0$ when $q_\perp$ cancels, whereas the frequency of the amplitude mode is different from zero at $q_\mathrm{s}=2q_0$, but has a minimum because of the contribution of the $2\alpha(T-T_\mathrm{c})/\eta$ term of relationship (1). So, the difference in temperature dependence of the above relationships leads us to expect different viscoelastic behaviour when the temperature changes.

3. Experimental

The material used here is the C_8tolane, which exhibits a ferroelectric phase (SmC*) between 97 and 104°C [15, 16]. The chemical formula and phase sequence were given in ref. [9]. C_8tolane, which is a powder at ambient temperature, was heated to the isotropic phase and then introduced by capillary action between two treated glass plates 100 µm apart. The glass plates were treated with octadecylsilane (ODS), $C_{18}H_{37}SI(OCH_3)$, which induces a homeotropic orientation. The glass plate treatment and the slow cooling ($0.01^\circ C\,min^{-1}$) from isotropic to SmC* phase gave a good homogeneous homeotropic orientation, with the helix axis normal to the glass plates. The homeotropic orientation state was cheked with an optical microscope with the sample placed between crossed polarizer and analyser. When homeotropic orientation was obtained no transmitted light could be observed in the optical microscope. An electric regulator fixed the sample temperature at 100°C.

To analyse the viscoelastic behaviour of C_8tolane in its SmC* phase we used the quasi-elastic light scattering technique; more precisely, the light beating technique that consists of measuring the autocorrelation function $C_i(t)$ of the photocurrent associated with light scattered by thermal collective fluctuations. In this method a 35 mW He-Ne laser beam ($\lambda = 6328$ Å) polarized vertically (the incoming electric field perpendicular to the incident plane: ordinary polarization) is used to illuminate the sample placed on a goniometer, allowing us to select an air incident angle in the range 18° to 33°. The scattered light passes through a pin-hole and is collected over a less-than-one coherence area by a cooled photomultiplier placed on a rotatable arm. This arm rotates around the vertical goniometer axis, to allow selection of the scattering angle. In front of the photomultipier a horizontal linear analyser is placed to collect the scattered light in an extraordinary polarization (the scattered electric field lies in the scattering plane).

The photocurrent provided by the photomultiplier is sent to a digital Flex01 correlator that gives the autocorrelation function $C_i(t)$ associated with the scattered light corresponding to thermal collective excitations. The measured $C_i(t)$ is then sent to a computer to be adjusted with a theoretical function $C_{ith}(t)$ given by the following expression:

$$C_{ith}(t) = A\exp(-t/\tau) + B\exp(-2t/\tau) + C$$

where τ is the relaxation time corresponding to the collective excitations of the considered mode. C is fixed to the measured base line. A and B are constants that depend essentially on experimental conditions: homodyne or heterodyne detections and coherence area number. For example, if the experiment is made in a purely heterodyne detection the constant B can be neglected. The comparison between A and B can thus give information about detection nature; the τ can be therefore deduced with more accuracy.

4. Results and discussion

The experimental results presented and discussed in this section are deduced from experiments performed on the SmC* phase of C_8tolane and concern only the analysis of scattered light corresponding to thermal collective fluctuations associated with the Goldstone mode. We should note that the Bragg reflection corresponding to the scattering wave vector $\vec{q}_0$ can not be observed by our experimental set-up which allows us to change the angle of incidence from 18° to 33°. We have therefore analysed the scattered light centered on 2 $\vec{q}_0$.

One can see easily that expression (2) involves contributions of both the purely twist fluctuations and the combination of splay and bend distortions. Therefore using appropriate scattering geometries, one can measure separately the relaxation times corresponding to twist mode and those corresponding to splay and bend deformations. Indeed the back scattering geometry is used to probe $\vec{q}$ along the helix axis, and the forward scattering geometry is used to probe $\vec{q}$ perpendicular to this axis. In figure (1), we present the scattering geometries in which the incoming beam and the scattered light are in ordinary and extraordinary polarizations, respectively (o, e).

Figure 1 (*a*), in which the scattering wave vector $\vec{q} = \vec{q}_s$ is kept closely parallel to the helix axis, allows us to measure the relaxation times associated with the Goldstone mode centred on the reflected beam; figure 1 (*b*) shows the scattering geometry in which $\vec{q}$ is normal to the helix axis, and allows us to measure the relaxation times corresponding to the combination of splay and bend fluctuations. Note that in such geometry, the incoming and scattered light are symmetric with respect to the helix axis.

Concerning purely twist deformations, we measured autocorrelation functions for several angles of incidence lying in the range 18°–33°, and then fitted them to exponential functions. The fit parameters give the amplitudes A and B and the damping times τ_p of the fluctuations in the SmC* phase. For most experiments, the ratio B/A is much less than 1%, which means that measurements of autocorrelation function associated with the scattered light intensity are performed in the heterodyne regime. This situation can be explained by the fact that in such a scattering geometry the scattered light is always mixed with some laser light because the detector is positioned very close to the reflected beam.

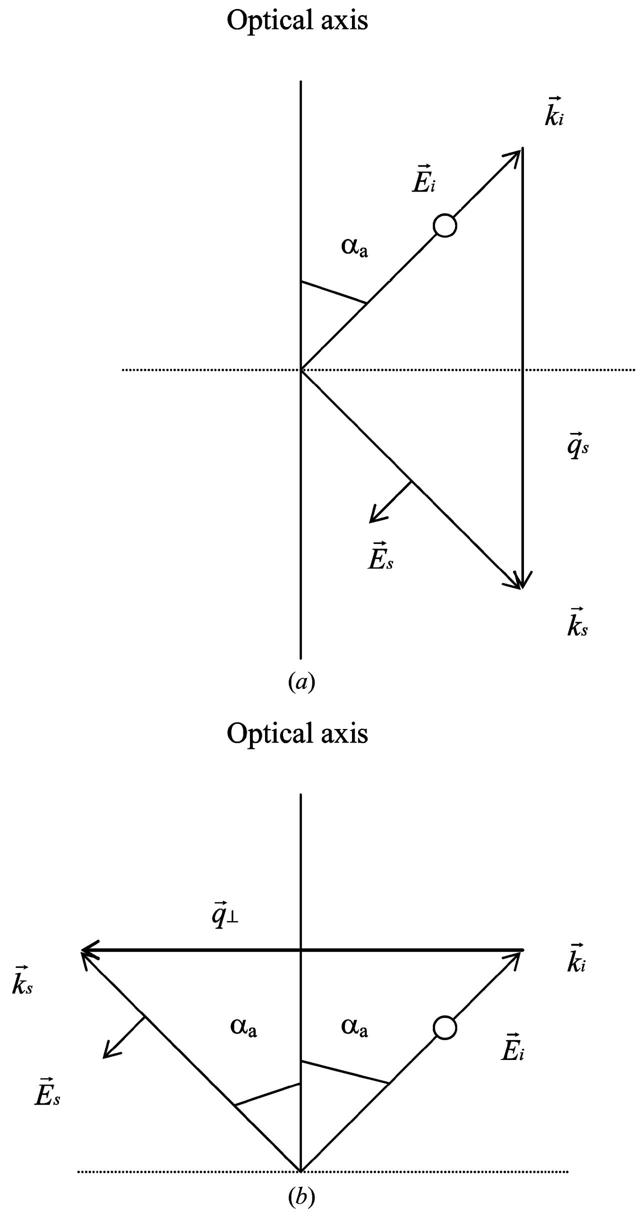

Figure 1. (*a*): Backward scattering geometry; (*b*) forward scattering geometry.

Figure 2 (*a*) shows the q_s dependence of the relaxation rate of the Goldstone mode observed at $2q_0$. The q_s values are obtained when we give the ordinary n_o and extraordinary n_e indices the values 1.50 and 1.69, respectively. These measurements were performed by our French group for the SmC* phase of C_8tolane. The best fit of experimental data is obtained by a parabolic function where the minimum is obtained at $q_s=2q_0=28.2\times10^4\,\mathrm{cm}^{-1}$. Note that the parabolic character is in good agreement with theoretical predictions — expression (2) — concerning the curve

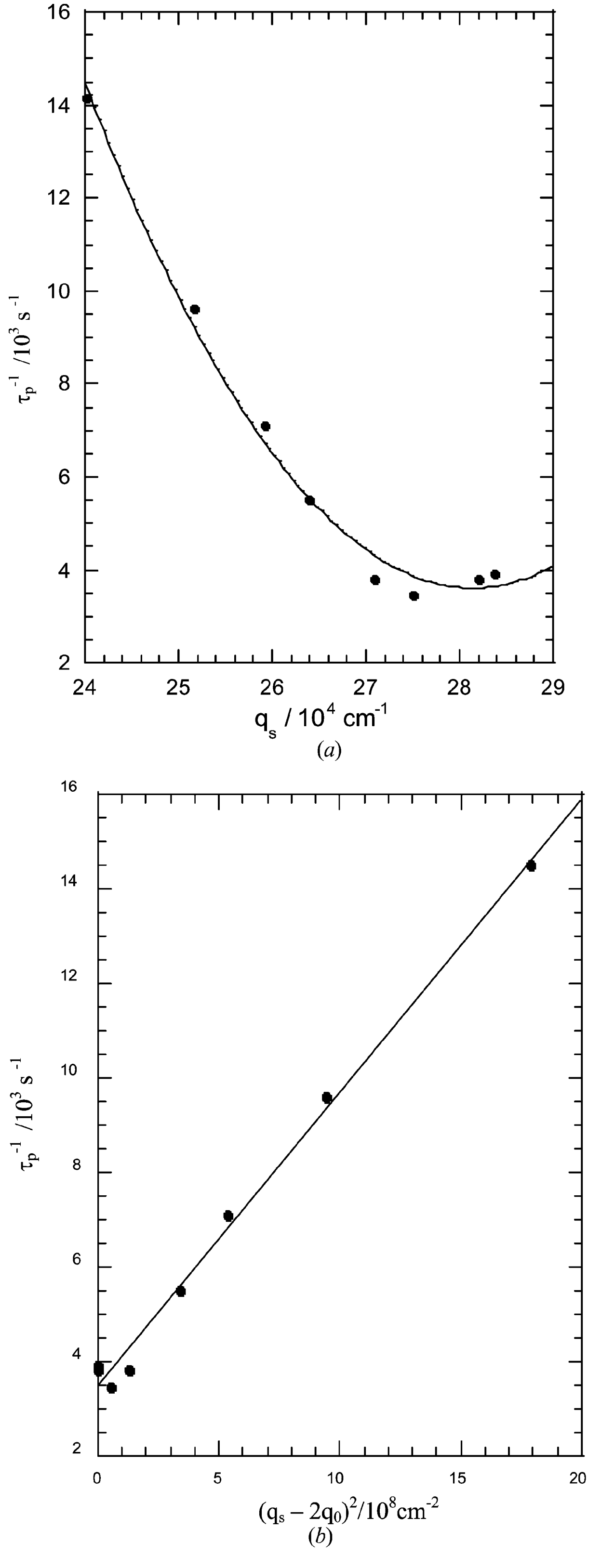

Figure 2. (*a*): Variation of relaxation rate τ_p^{-1} versus q_s in backward scattering geometry; (*b*) variation of relaxation rate τ_p^{-1} versus $(q_s-2q_0)^2$ in backward scattering geometry.

associated with the frequency dispersion branch of the Goldstone mode. From the value of q_0, one can deduce the helix pitch $p=0.45\,\mu m$ that agrees with selective reflection measurements [17]. The non-zero frequency of the relaxation rate dispersion observed at $q_s=2q_0$ can be attributed to the contribution of a small component $q_\perp$ due to a weak misalignment of q_s with respect to the helix axis.

In figure 2 (*b*), we plot relaxation rates dispersion versus $(q_s \pm 2q_0)^2$. The data are well fitted by a straight line. The corresponding slope gives the orientational diffusivity associated with the Goldstone mode: $D=k_3/\eta=6.2\times10^{-10}\,m^2\,s^{-1}$.

Using the forward scattering geometry presented in figure 1 (*a*), we measured the relaxation rates of thermal fluctuations corresponding to the combination of splay and bend deformations. The incidence angles were chosen in the range 1° to 14.5°. Because of experimental constraints, it was not possible to investigate the symmetric angles lying in the range −1° to −14.5°. Figure 3 (*a*) is a plot of the relaxation rate change τ_p^{-1} versus $q_\perp$, where the parabolic dependence expected theoretically is found when q_s is zero. The change of relaxation rate versus $q_\perp^2$ is presented in figure 3 (*b*); a straight line gives the best fit for the experimental data. The corresponding slope gives $k_+/\eta=3.6\times10^{-9}\,m^2\,s^{-1}$, while the frequency at $q_\perp=0$ corresponds to $4k_3q_0/\eta=5.5\times10^4\,Hz$. If we give q_0 the value $14.1\times10^4\,cm^{-1}$ found above, we deduce $k_3/\eta=7\times10^{-11}\,m^2\,s^{-1}$ which is about one tenth of that derived from the backward scattering geometry. This difference can be explained by: (*i*) in the forward scattering geometry, only the positive incidence angle range has been investigated, which can induce an uncertainty in the determination of the parabolic function minimum; (*ii*) the contribution of a small component q_s due to an uncertainty of the detector position can also induce errors, so that the scattering wave vector is not exactly normal to the helix axis.

To compare the viscoelastic behaviour of ferro- and antiferro-electric liquid crystal phases, we report in the table results deduced from this study and those deduced from previous investigations [9]. Within the limits of experimental error, we note that for the same liquid crystal (C_8tolane) the orientational diffusivity k_3/η measured in the SmC$_A^*$ phase is about 100 times weaker than the one measured in the SmC* phase. The same behaviour has been observed in C_{11}thiobenzoate. This result means that ferro- and antiferro-electric phases (SmC* and SmC$_A^*$) of the same liquid crystal (C_8tolane or C_{11}thiobenzoate) do not present the same viscoelastic behaviour. The difference can thus be attributed largely to the difference in molecular arrangement in these

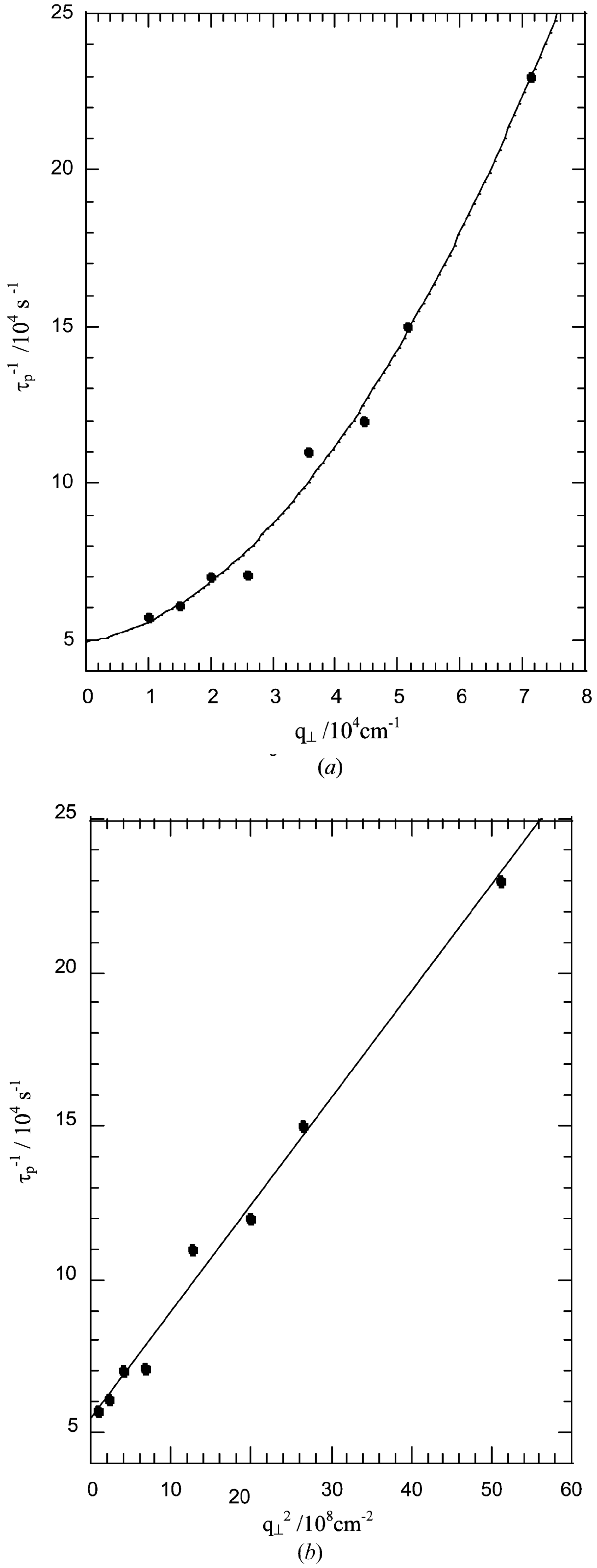

Figure 3. (*a*): Variation of relaxation rate τ_p^{-1} versus $q_\perp$ in forward scattering geometry; (*b*) variation of relaxation rate τ_p^{-1} versus $q_\perp^2$ in forward scattering geometry.

Table. Orientational diffusivities corresponding to purely twist deformations and the combination of splay and bend distortion.

Sample	Phase	$\frac{k_3}{\eta}$/m^2 s^{-1}	$\frac{k_+}{\eta}$/m^{2}s^{-1}
C_8tolane	SmC_A*	1.3×10^{-12}	$\approx10^{-7}$
	SmC*	6.2×10^{-10}	3.6×10^{-9}
C_{11}thiobenzoate	SmC_A*	2×10^{-11}	$\approx10^{-8}$
	SmC*	7×10^{-9}	—

phases. Note that in this study we have investigated only the SmC* phase of C_8tolane in order to support explanations and arguments given in [9]; more details on the viscoelastic behaviour of the SmC_A^* phase are presented in this reference.

Orientational diffusivities k_+/η deduced from backward and forward scattering are almost in the same order of magnitude except for k_+/η for to the SmC* phase of C_8tolne, which seems to be weaker than the others. The deviation can be attributed to experimental errors, particularly to the uncertainty in determination of the zero frequency at $q_\perp=0$, because in forward scattering only the positive angles range has been investigated, so that the parabolic function minimum could not be determined with good precision.

5. Conclusion

Using light scattering techniques, we have investigated the viscoelatic behaviour exhibited by the ferroelectric phase (SmC*) of C_8tolane liquid crystal at a fixed temperature of 100°C. More precisely, we have measured the autocorrelation function corresponding to scattered light intensity associated with collective excitations of the Goldstone mode. Experiments were performed in backward and forward scattering geometries which allowed us to deduce separately orientational diffusivities k_3/η and k_+/η associated with purely twist deformations and the combination of splay and bend distortion, respectively.

A comparison between results presented here and previously [9] shows that k_3/η values measured in SmC_A^* phases are about 100 times weaker than those k_3/η measured in SmC* phases. The factor 100 is attributed largely to 'molecular arrangement modes' observed in these phases. Thus, the viscoelastic behaviour of ferro- and antiferro-electric phases is governed by the molecular arrangement mode in adjacent smectic layers. On the other hand, and within the limits of experimental error, orientational diffusivities k_+/η corresponding to SmC_A^* and SmC* phases are almost in the same order of magnitude and agree with those measured previously by other authors.

References

[1] R.B. Meyer, L. Liebert, L. Strzlecki, P. Keller. *J. Phys. Lett.*, **36**, 169 (1975).

[2] A.M. Levelut, C. Germain, P. Keller, L. Liebert, J. Billard. *J. Phys.*, **44**, 623 (1983).

[3] Y. Galerne, L. Liebert. *Phys. Rev. Lett.*, **64**, 906 (1990).

[4] A.D.L. Chandani, E. Gorecka, Y. Ouchi, H. Takezoe, A. Fukuda. *Jpn. J. Appl. Phys.*, **28**, 1265 (1989).

[5] C. Bahr, D. Fliegner. *Phys. Rev. Lett.*, **70**, 1842 (1993).

[6] C. Bahr, D. Fliegner. *Ferroelectrics*, **147**, 1 (1993).

[7] M.O. Freeman, T.A. Brown, D.M. Walba. *Appl. Opt.*, **31**, 3917 (1992).

[8] N.A. Clark, S.T. Lagerwall. *Appl. Phys. Lett.*, **36**, 899 (1980).

[9] T. Othman, Z. Hammami, A. Gharbi, H.T. Nguyen. *Liq. Cryst.*, **31**, 1061 (2004).

[10] T. Othman, M. Gharbia, A. Gharbi, C. Destrade, G. Durand. *Liq. Cryst.*, **18**, 938 (1995).

[11] E. Gorecka, A.D.L. Chandani, Y. Ouchi, H. Takazoe, A. Fukuda. *Jpn. J. Appl. Phys.*, **29**, 131 (1990).

[12] K. Hiraoka, H. Takazoe, A. Fukuda. *Ferroelectrics*, **13**, 147 (1993).

[13] S. Yuyvaraj, K.A. Suresh. *Liq. Cryst.*, **24**, 701 (1998).

[14] I. Drevensek, I. Musevic, M. Copic. *Phys. Rev. A*, **41**, 923 (1990).

[15] H.T. Nguyen, J.C. Rouillon, P. Cluseau, G. Sigaud, C. Destrade, N. Isaert. *Liq. Cryst.*, **17**, 571 (1994).

[16] A. Bouchta, H.T. Ngyuen, L. Navalles, P. Barois, C. Destrade, F. Bougrioui, N. Isaert. *J. mater. Chem.*, **5**, 2079 (1995).

[17] P. Cluseau. PhD thesis, Centre de Recherche Paul Pascal-, Bordeaux, France (1995).